Letter

Cut structures and an observable singularity in the three-body threshold dynamics: The T_{cc}^+ case

Jun-Zhang Wang,* Zi-Yang Lin,† and Shi-Lin Zhu‡

School of Physics and Center of High Energy Physics, Peking University, Beijing 100871, China

(Received 18 January 2024; accepted 28 March 2024; published 25 April 2024)

The three-body threshold effect, the distinctive and intriguing nonperturbative dynamics in the low-energy hadron-hadron scattering, has acquired compelling significance in the wake of the recent observation of the double-charm tetraquark T_{cc}^+. This dynamics is characterized by the emergence of singular points and branch cuts within the interaction potential, occurring when the on-shell condition of the mediated particle is satisfied. The presence of these potential singularities indicates that the system is no longer Hermitian and also poses intractable challenges in obtaining exact solutions for dynamical scattering amplitudes. In this work, we develop a complex scaled Lippmann-Schwinger equation as an operation of analytical continuation of the T matrix to resolve this problem. Through a practical application to the $DD^* \to DD^*$ process, we reveal complicated cut structures of the three-body threshold dynamics in the complex plane, primarily stemming from the one-pion exchange. Notably, our methodology succeeds in reproducing the T_{cc}^+ structure, in alignment with the quasibound pole derived from the complex scaling method within the Schrödinger equation framework. More remarkably, after solving the on-shell T matrix on the positive real axis of momentum plane, we find an extra new structure in the DD^* mass spectrum, which arises from a right-hand cut at a physical pion mass and should be observable in lattice QCD simulations and future high-energy experiments.

DOI: 10.1103/PhysRevD.109.L071505

Introduction. Low-energy hadron-hadron interactions offer a window into the nonperturbative dynamics of the fundamental theory of the strong force, i.e., quantum chromodynamics (QCD), which has been one of the most important issues in particle physics and nuclear physics. Due to the color confinement of QCD, theorists have come to realize that hadrons can be treated as an effective basic freedom in the low-energy strong interaction. Thus, a modern advanced tool of effective field theory has been proposed to describe these interactions, such as the chiral perturbation theory (ChPT) based on the spontaneous breaking of chiral symmetry in QCD [1–11]. In the framework of the effective field theory, the strong force is mediated by the exchange of mesons, particularly pions. A representative example is the nucleon-nucleon interaction, the attractive and repulsive behaviors of which are pivotal for comprehending nuclear forces and atomic nucleus properties [9,10].

*wangjzh2022@pku.edu.cn
†lzy_15@pku.edu.cn
‡zhusl@pku.edu.cn

The exciting advancement in the realm of low-energy strong interactions still continues. Very recently, the LHCb Collaboration observed a double-charm exotic hadron T_{cc}^+ in the mass spectrum of $D^0D^0\pi^+$ [12,13], in which the extracted pole information is given by

$$\delta m_{\text{pole}} = -360 \pm 40\,\text{keV}, \quad \Gamma_{\text{pole}} = 48 \pm 2\,\text{keV}, \quad (1)$$

with a unitarized Breit-Wigner parametrization scheme [13]. Here, $\delta m = m - m_{D^0} - m_{D^{*+}}$. It is evident that the pole position of T_{cc}^+ lies in extremely close proximity to the D^0D^{*+} threshold. Consequently, this state has commonly been regarded as a good candidate of a heavy-flavored hadronic molecule, formed through the interaction of charmed mesons DD^* [14–38]. Undoubtedly, the discovery of T_{cc}^+ offers an exceptional opportunity to illuminate the intricate internal dynamics of the hadron-hadron interactions involving heavy quarks.

Similar to the nucleon-nucleon interactions, the heavy-meson-heavy-meson interactions share a common underlying dynamics characterized by the exchange of pions and heavier isoscalar mesons. However, a unique aspect of the DD^* interaction is the inherent instability of the D^* meson, leading to its decay into $D\pi$ and the possibility of introducing an on-shell intermediate pion meson in the pion-exchange interactions. At the leading order, this

on-shell singularity appearing in the one-pion-exchange (OPE) potential, results in a nonvanishing imaginary component and renders the Hamiltonian non-Hermitian. According to the optical theorem, this imaginary part of the OPE potential corresponds to the three-body $DD\pi$ decay. Importantly, the final $DD\pi$ states is the sole strong decay mode of T_{cc}^{+}. This underscores the critical role of the three-body dynamics in unveiling the nature of the special T_{cc}^{+} state. In previous works [27,28], a revised OPE potential incorporating the three-body threshold dynamics within a relativistic pion propagator has been achieved, which effectively explains the observed narrow width of the T_{cc}^{+} state.

In the context of the OPE potential involving the three-body dynamics, in addition to a unitary cut at the three-body threshold, more plentiful cut structures exist, which potentially give rise to intriguing physical phenomena. In this work, we systematically study the cut structures of the three-body threshold dynamics in the complex plane, which include the cases of the on-shell amplitudes and half-on-shell amplitudes when opening or closing the three-body dynamics. Subsequently, we concentrate on the situation of interest to us in which the three-body threshold dynamics is active, and find that the branch cut of the half-on-shell amplitude with an imaginary on-shell momentum always traverses the positive real axis, which may lead to unavailability of the conventional Lippmann-Schwinger equation in obtaining the physical on-shell T matrix below the energy threshold. In order to resolve this problem, we develop a complex scaled Lippmann-Schwinger equation (CSLSE) approach, which ensures a logical treatment of analytical continuation of the T matrix. Additionally, the another advantage of this method is its high efficiency in addressing the divergence issue associated with the double singular points of the potential function along the integral path when computing the physical on-shell T matrix above the energy threshold. By taking the isoscalar DD^* scattering as an example, the observed quasi-bound T_{cc}^{+} structure in LHCb can be clearly reproduced in the CSLSE. More intriguingly, we find an extra new structure in the DD^* mass spectrum for the first time by solving the physical on-shell T matrix above the energy threshold, which can be tested in lattice simulations.

Cut structures in the analytical extension of the three body $DD\pi$ dynamics. In the heavy meson chiral effective field theory (HMChEFT) [11], the leading order interactions of the $DD^* \to DD^*$ scattering include the contact term and OPE potential. In order to introduce the three-body threshold dynamics (see Supplemental Material [39] for more details), the S-wave OPE interaction of the isoscalar DD^* state ($I=0$) can be revised as

$$V_{\rm OPE}^{I=0} = -\frac{g^2}{8f_\pi^2}\frac{(p^2+p'^2-2pp'z)(\varepsilon'\cdot\varepsilon)}{(E'+\delta)^2-(p^2+p'^2-2pp'z)-m_\pi^2+i\epsilon}, \tag{2}$$

where the center-of-mass kinetic energy $E'=k_0^2/(2\mu)$ and $\delta = m_{D^*}-m_D$. We further define an effective mass square $m_{\rm eff}^2=(E'+\delta)^2-m_\pi^2$. Based on this definition, the pion propogator in Eq. (2) can be written as $1/(m_{\rm eff}^2-\boldsymbol{q}^2)$. It can be seen that when $m_{\rm eff}^2>0$, there appears an infinity for $\boldsymbol{q}^2=m_{\rm eff}^2$, which will induce a three-body $DD\pi$ cut and there are no singularities in the real momentum range for the case of $m_{\rm eff}^2<0$. For the S-wave scattering process, the partial-wave-projected components of its total potential can be obtained by

$$V_S^{I=0}(p,p') = 4\pi C_t + \int_{-1}^{1} dz 2\pi V_{\rm OPE}^{I=0}(p,p',z). \tag{3}$$

As the scattering amplitude of the leading-order Born approximation, $V_S^{I=0}(p,p')$, does not satisfy the unitarity. In order to ensure the unitarity and produce bound states, resonances or virtual states [40], the resummation via a dynamical equation is needed. For the two-particle system, its dynamical scattering can be described by the Lippmann-Schwinger equation (LSE) or Schrödinger equation. The LSE is given by

$$T_{\alpha\beta}(p,p',k_0) = V_{\alpha\beta}(p,p',k_0) + \sum_\gamma \int_0^\infty \frac{dqq^2}{(2\pi)^3} V_{\alpha\gamma}(p,q,k_0) \times G_\gamma(q,k_0) T_{\gamma\beta}(q,p',k_0), \tag{4}$$

with

$$G_\gamma(q,k_0) = \frac{2\mu_\gamma}{k_0^2-q^2+i\epsilon}, \tag{5}$$

where $V_{\alpha\beta}(p,p',k_0)$ is the partial-wave-projected potential of the α channel to the β channel, and p and p' correspond to the initial and final momentum, respectively. It is worth mentioning that the angular integration in LSE has been absorbed in the partial-wave projected interaction potential $V_{\alpha\beta}(p,p',k_0)$ as performed in Eq. (3). The center-of-mass momentum k_0 and the reduced mass μ_γ are defined by

$$k_0^2 = 2\mu_\gamma(E-m_1-m_2), \qquad \mu_\gamma = \frac{m_1 m_2}{m_1+m_2}. \tag{6}$$

Considering a single channel case $DD^* \to DD^*$ ($I=0$), the Green's function in the dynamical equation includes a right-hand unitary cut from the two-body threshold, i.e., $k_0^{\rm Rh} = \sqrt{2\mu(m_D+m_{D^*})}$.

However, the partial-wave OPE potential involving the three-body dynamics will induce a new cut structure. For the on-shell scattering amplitude ($p=p'=k_0$), the position of this branch point can be derived from Eq. (3), i.e.,

$$(k_0)^2 = m_{\rm eff}^2/4 = \left((E'+\delta)^2-m_\pi^2\right)/4.$$

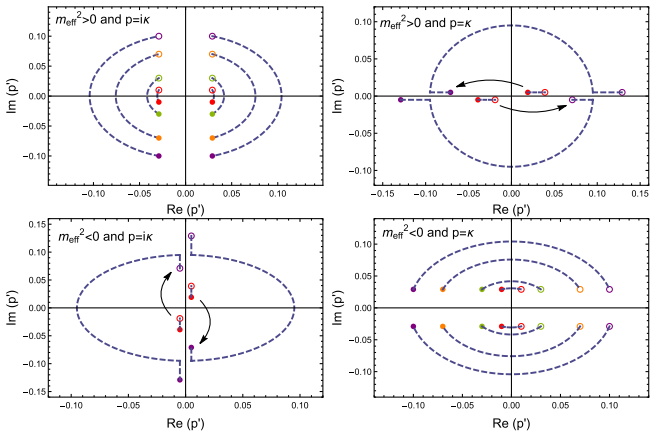

FIG. 1. The cut structures of the half-on-shell scattering amplitudes from the OPE potential involving the three-body dynamics under different cases. The red, green, orange and purple singularities correspond to $\kappa = 0.01$, 0.03, 0.07 and 0.1 GeV, respectively and the dashed line denotes the branch cuts.

When $m_{\rm eff}^2 < 0$, which could correspond to a larger unphysical pion mass, the three-body threshold is not enabled. This cut becomes a left-hand cut below the energy threshold. However, for a physical m_π ($m_{\rm eff}^2 > 0$), it can be expected that there exists a right-hand cut above the DD^* threshold.

In fact, we can further make an analytical continuation of the potential $V_S^{I=0}(p, p')$ to study the cut structures of the three-body dynamics in the complex plane, which is usually related to the half-on-shell scattering amplitude ($k_0 = p$). The behaviors of their singularities (branch points) and branch cuts are obviously distinct according to the signs of k_0^2 and $m_{\rm eff}^2$, which are shown in Fig. 1 by taking the constant $m_{\rm eff}^2 = \pm 8.43 \times 10^{-4}$ GeV^2 (ignore the dependence of k_0 in $m_{\rm eff}^2$) as an example. Here, this absolute value of $m_{\rm eff}^2$ is obtained by the input of $m_D = 1.867, m_{D^*} = 2.009$, $m_\pi = 0.139$ GeV. The main contents and conclusions of four cases are summarized

(i) For the case of $m_{\rm eff}^2 > 0$, which corresponds to the physical pion mass, and center-of-mass energy E below the threshold ($k_0 = p = i\kappa$ with real κ), it has four branch points $(m_{\rm eff} + i\kappa)$, $(m_{\rm eff} - i\kappa)$, $(-m_{\rm eff} + i\kappa)$ and $(-m_{\rm eff} - i\kappa)$ in the complex plane of p'. It can be found that the branch cuts are transversely symmetrical and the path along the real axis will encounter branch cuts.

(ii) For the case of $m_{\rm eff}^2 > 0$ and E above the threshold ($k_0 = p = \kappa$ with real κ), it has four branch points $(\kappa + m_{\rm eff} + i\epsilon)$, $(\kappa - m_{\rm eff} - i\epsilon)$, $(-\kappa + m_{\rm eff} + i\epsilon)$ and $(-\kappa - m_{\rm eff} - i\epsilon)$ on the real axis. When κ is relatively small, its branch cut is a line segment. However, an interesting phenomenon is that each of the two branch points near the origin crosses the imaginary axis and moves to the opposite half-plane as κ gradually increasing till a critical point $\kappa = |m_{\rm eff}|$. At this point the branch cut will change drastically, whose closed behavior covers almost every possible path from the origin. It is worth noting that the real axis is the only path which does not encounter branch cuts after considering an infinitesimal imaginary part $i\epsilon$.

(iii) For the case of $m_{\rm eff}^2 < 0$, which is usually related to the unphysical pion mass as in lattice QCD simulation, and E below the threshold, it has four branch points $((\kappa + m_{\rm eff})i + \epsilon)$, $((\kappa - m_{\rm eff})i - \epsilon)$, $((-\kappa + m_{\rm eff})i + \epsilon)$ and $((-\kappa - m_{\rm eff})i - \epsilon)$ on the imaginary axis. As κ increases, the behaviors of the branch points are similar to the above case. The only difference is that they are aligned along the imaginary axis. The imaginary axis is the only path which will not encounter branch cuts when $\kappa > |m_{\rm eff}|$.

(iv) For the case of $m_{\rm eff}^2 < 0$ and E above the threshold, it has four branch points $(\kappa + im_{\rm eff})$, $(\kappa - im_{\rm eff})$, $(-\kappa + im_{\rm eff})$ and $(-\kappa - im_{\rm eff})$. It can be found that the branch cuts are longitudinally symmetrical and the path along the real axis will not encounter branch cuts.

The complex scaled Lippmann-Schwinger equation. Due to the intricate cut structures arising from the three-body $DD\pi$ effect, its dynamical resummation within the framework of LSE is also expected to be more complicated. The conventional Lippmann-Schwinger equation is

$$T(p, p', k_0) = V(p, p', k_0) + \int_0^\infty \frac{dqq^2}{(2\pi)^3} V(p, q, k_0) \times G(q, k_0) T(q, p', k_0), \tag{7}$$

where the integral path along the loop momentum q follows a physical positive real axis. For the solution of the on-shell T matrix with E below the threshold and physical pion mass, as depicted in Fig. 1, it is evident that the path along real axis always intersects the branch cut of the potential. Such a phenomenon does not happen in the case of the on-shell T matrix with E above the threshold. Additionally, for $V(p, q, k_0) = V_{S,\rm OPE}^{I=0}(\kappa, q, \kappa)$ with physical pion mass, as shown in Fig. 1, it introduces two singular points precisely on the integral path along the positive real axis, and the resulting divergence poses challenges in accurately computing the on-shell amplitude $T(\kappa, \kappa, \kappa)$ using the dynamical equation. Although it is still feasible to directly encompass the contribution of this divergence using an alternative scheme within the conventional LSE framework (as detailed in the Supplemental Material [39]), such a formalism demands sufficiently high numerical accuracy.

In this work, we develop a complex scaled Lippmann-Schwinger equation to effectively address these issues and challenges brought about by the cut structures of the three-body dynamics. One significant advantage of this approach lies in its remarkable efficiency in resolving the divergence

issue associated with the singular points in both the potential and Green's function. In order to avoid the singularities of the potential, one can extend the integral path of the LSE to the complex plane to ensure an identical integral result. Let us begin with the case involving a physical pion mass. When $p = \kappa$ is not larger than the critical point $\kappa = |m_{\rm eff}|$, the branch cut locates on real axis. Then a complex scaling rotation transformation $q \to qe^{-i\theta}$ is introduced and the LSE becomes

$$T(p,p',k_0)=V(p,p',k_0)+\int_0^\infty \frac{dqq^2}{(2\pi)^3}e^{-i3\theta} \times V(p,qe^{-i\theta},k_0)G_\gamma(qe^{-i\theta},k_0)T(qe^{-i\theta},p',k_0). \tag{8}$$

However, for $p > |m_{\rm eff}|$, this path will cross the circular branch cut and enter another Riemann surface of the potential function and thus is no longer applicable. Hence, the only available integral path is along the positive real axis. On the unphysical pion mass conditions, the situation becomes more manageable because the singular points of the potential are distant from the real axis. Moreover, the complex scaled path remains applicable and offers a distinct benefit by automatically incorporating the discontinuity component from the Green's function. A more detailed discussion can be found in Supplemental Material [39]. It is worth emphasizing that the LSE in Eq. (8) is no longer an iterative equation and cannot be directly solved. Therefore, a key issue revolves around the analytical continuation of the T matrix.

In Fig. 2, we show the evolution of the branch points of the OPE potential involving the three-body dynamics in the complex plane when performing a complex scaling transformation $p = \kappa \to \kappa e^{-i\phi}$ and $p = \kappa \to \kappa e^{i\phi}$. For the clockwise transformation $p = \kappa e^{-i\phi}$, the hollow circle branch points move to the lower half-plane and solid circle branch points move to the upper half-plane, and vice versa. From Fig. 2, it is evident that certain branch points will traverse the positive real axis, consequently altering the relative positioning of the branch points with respect to the integral path along the positive real axis. To maintain analyticity and continuity of the T matrix when extending it to the complex plane, a complex scaling transformation should also be applied to the integral path in LSE. For the clockwise transformation, the complex scaled Lippmann-Schwinger equation (CSLSE) can be written as

$$T(\kappa e^{-i\phi},p',k_0) = V(\kappa e^{-i\phi},p',k_0) + \int_0^\infty \frac{dqq^2}{(2\pi)^3}e^{-3i\phi} \times V(\kappa e^{-i\phi},qe^{-i\phi},k_0) \times G_\gamma(qe^{-i\phi},k_0)T(qe^{-i\phi},p',k_0), \tag{9}$$

where $T(\kappa e^{-i\phi},p',k_0)$ can be numerically solved through an iterative equation. For the counterclockwise

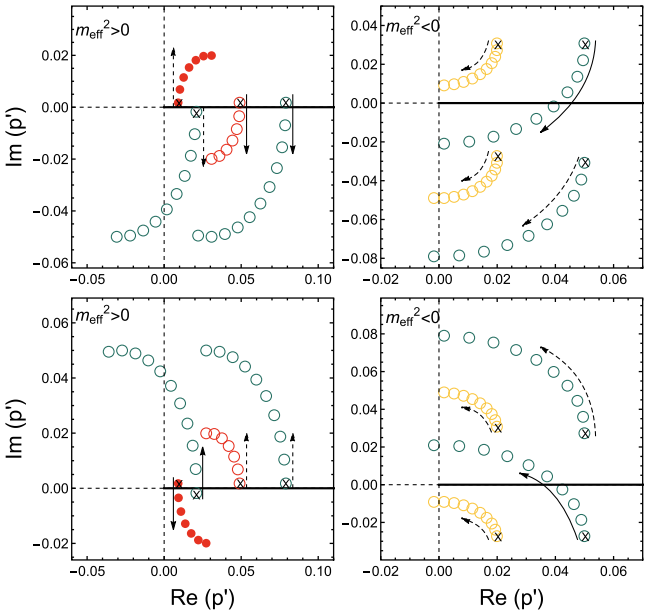

FIG. 2. The evolution of the branch points in the OPE potential with the three-body dynamics using complex scaling transformations: $p = \kappa \to \kappa e^{-i\phi}$ (upper plot) and $p = \kappa \to \kappa e^{i\phi}$ (lower plot). The red (yellow) and green points correspond to $\kappa = 0.01$ and 0.1 GeV, respectively, and points with the cross mark denotes $\phi = 0°$.

transformation $p = \kappa \to \kappa e^{i\phi}$, the corresponding analytical continuation will become complicated. For $\kappa < |m_{\rm eff}|$ on the physical pion mass condition, the solid circle branch point will traverse the positive real axis when $p = \kappa \to \kappa e^{i\phi}$. The transformation of the integral path should be $q \to qe^{-i\phi}$ instead of $q \to qe^{i\phi}$ and the corresponding CSLSE is

$$T(\kappa e^{i\phi},p',k_0) = V(\kappa e^{i\phi},p',k_0) + \int_0^\infty \frac{dqq^2}{(2\pi)^3}e^{-3i\phi} \times V(\kappa e^{i\phi},qe^{-i\phi},k_0)G_\gamma(qe^{-i\phi},k_0) \times T(qe^{-i\phi},p',k_0). \tag{10}$$

While κ exceeds a critical point, the hollow circle branch point, originating from the negative real axis as shown in Fig. 2, can cross the positive real axis and move faster than the rotational transformation. As a result, a logical path transformation of $q \to qe^{-i(180-\phi)}$ should be carried out. The similar conclusion can also be reached for a large κ on an unphysical pion mass condition. Finally, it is worth noting that the analytic continuation operations mentioned above require simultaneously ensuring the continuity of the integrated T matrix.

Through the CSLSE approach, a half-on-shell T matrix $T(pe^{i\theta},k_0,k_0)$ can be derived, which can be subsequently reintroduced into the integral in Eq. (8) by setting $p = p' = k_0$. This allows for the successful calculation

of the physical on-shell T matrix. Of course, one of the most important deduction derived from the CSLSE is that the on-shell T matrix below the energy threshold $T(i\kappa, i\kappa, i\kappa)$ should be computed using the integral path near the negative imaginary axis, just as $i\kappa$ corresponds to $\phi = 90°$. This implies that a straightforward extension of $p \to i\kappa$ in the conventional LSE in Eq. (7) may be inadequate for dealing with this special interaction involving the three-body dynamics. This insight will be substantiated through a practical example later.

Applications and conclusion. We now present a practical calculation of the isoscalar DD^* scattering with the isospin symmetry by the CSLSE approach. In order to validate the reliability of our computed results, we focus on the pole information of T_{cc}^+, which was previously investigated in Ref. [27] using the complex scaling method for Schrödinger equation. This method does not involve the branch cut complexities of the three-body dynamics and conveniently allows us to extract the dynamical pole position. Since ChEFT only works at the small momentum regions and the CSLSE also requires the convergence at infinity of the integral, a Gaussian form factor is introduced to regularize the effective potential, which reads

$$\mathcal{F}(p, p') = \exp\left[-\frac{p^2}{\Lambda^2} - \frac{p'^2}{\Lambda^2}\right]. \tag{11}$$

The physical on-shell T matrix of the isoscalar DD^* scattering below the threshold are shown in Fig. 3, in which two different integral paths are adopted, i.e., the positive real axis and negative imaginary axis, which correspond to the path of crossing and not crossing the branch cut, respectively, as shown in Fig. 1. In fact, there is flexibility to choose alternative rotation angles according to the Cauchy integral theorem, as long as the chosen paths consistently conform to either crossing or avoiding the branch cut. In the specific scenario, we have confirmed that the computation results are independent of the choice of the rotation angle.

From Fig. 3, it can be seen that the line shape distribution of the T_{cc}^+ state in the scattering amplitude can be accurately replicated, with the pole information matching that obtained through the complex scaling method of the Schrödinger equation [27]. This provides compelling evidence for the validity of the CSLSE approach. Furthermore, we find that there is an unexpected divergency of the T matrix at the two-body threshold for the integration scenario along the positive real axis, which is not caused by the precision of numerical calculation. A proof is presented as follows,

$$V_{\rm OPE}^{I=0}(i\kappa, p) \propto \frac{\mathrm{Log}(1 + (4\kappa p i)/(p^2 - 2\kappa p i - m_{\rm eff}^2 + i\epsilon))}{\kappa p}, \tag{12}$$

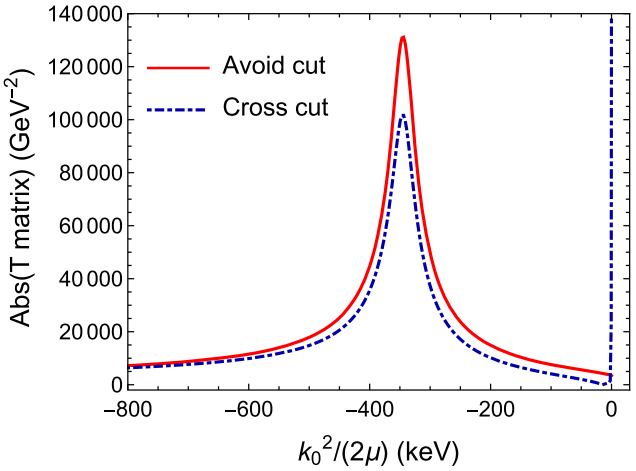

FIG. 3. The physical on-shell T matrix of the isoscalar DD^* scattering below the threshold.

when $\kappa \sim \epsilon$ is a small quantity (close to the threshold). In the limit of $\kappa \to 0$, if the value of momentum p traverses the branch cut, this expression can be further simplified as

$$V_{\rm OPE}^{I=0}(i\kappa, p) \propto \frac{-4i}{(m_{\rm eff}^2 - p^2 - i\epsilon)} - \frac{2\pi i}{\kappa p} \tag{13}$$

$$\sim \frac{(2\pi i)}{\kappa p} \to \infty. \tag{14}$$

Obviously, this divergency at the DD^* threshold should be unphysical. Hence, this point reinforces our conclusion that the accurate solution of the physical on-shell T matrix below the threshold should be conducted within the CSLSE framework.

Furthermore, we calculate the physical on-shell T matrix of the isoscalar DD^* scattering above the threshold, which is presented in Fig. 4. Very interestingly, the obtained T matrix shows the existence of an extra new structure in addition to the reported T_{cc}^+ state. This new structure is due to the right-hand cut effect of the OPE potential involving the three-body dynamics. In order to further test our theoretical predictions, we also study the dependence on the cutoff parameter by changing Λ between $0.5 \sim 0.7$ GeV. The existence of this structure is robust as shown in Fig. 4. The detection of this enhancement in experiments may necessitate the on-shell DD^* beam scattering, a technology that could be explored in future high-energy experiments. In the current experimental setup involving the inclusive DD^* production [12,13], detecting this structure is challenging since the initial DD^* is unnecessarily on-shell. From another perspective, the promising validation of this structure can be pursued through Lattice QCD simulations. In recent years, several lattice groups have already studied DD^* scattering at different nonphysical pion masses [41–46]. We notice that the recent study of HAL QCD on T_{cc}^+ has extracted the

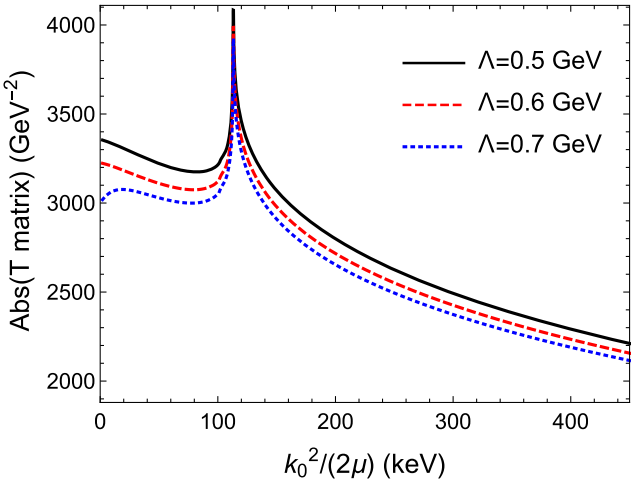

FIG. 4. The physical on-shell T matrix of the isoscalar DD^* scattering above the threshold.

S-wave scattering phase shifts of the DD^* scattering at a nearly physical pion mass $m_\pi = 146.4$ MeV [46]. The S-wave scattering phase shift δ_0 is directly related to the on-shell $T(k_0)$ matrix by

$$k_0 \cot\delta_0 = -\frac{8\pi^2}{\mu} T^{-1}(k_0) + ik_0. \tag{15}$$

The phase shift $k_0 \cot\delta_0/m_\pi$ obtained by lattice QCD confirms a linear relationship with the variable k_0^2/m_π^2 [46]. This behavior can be ascribed to the lack of the three-body dynamics at an unphysical pion mass $m_\pi = 146.4$ MeV used in their lattice simulations, where the trivial interaction enables the representation of the T matrix through the effective range expansion, i.e., $T^{-1} \propto (1/a_0 + 1/2rk_0^2)$. Interestingly, when the three-body threshold dynamics is activated, the $k_0 \cot\delta_0/m_\pi$ is no longer pure real numbers and the linear relation of its real part with the k_0^2/m_π^2 is seriously distorted (see predicted results in Supplemental Material [39]). This newly predicted structure arising from the right-hand cut is also manifested in both the real and imaginary parts of $k_0 \cot\delta_0/m_\pi$, providing an opportunity for future verification through Lattice QCD simulations.

In conclusion, we have developed a complex scaled Lippmann-Schwinger equation to address the complicated three-body threshold dynamics in low-energy hadron-hadron scatterings. The methodology is practically applied to the isoscalar DD^* scattering process under a physical pion mass, and succeeds in reproducing the T_{cc}^+ structure, aligned with the pole derived from the complex scaling method in the Schrödinger equation framework. Moreover, by solving the on-shell T matrix along the positive real axis of the momentum plane, a new structure stemming from a right-hand cut in the DD^* mass spectrum is discovered for the first time. It is worth emphasizing that a similar novel structure is expected to exist in other systems such as $D\bar{D}^*, \Lambda_c\Sigma_c^{(*)}, \Lambda_c\bar{\Sigma}_c^{(*)}$, and more, serving as a distinctive indicator and presenting a valuable opportunity to explore the role of the three-body threshold dynamics in low-energy heavy-hadron-heavy-hadron interactions.

Acknowledgments. This work is supported by the National Science Foundation of China under Grants No. 11975033, No. 12070131001 and No. 12147168. J. Z. W. is also supported by the National Postdoctoral Program for Innovative Talent. The authors thank Lu Meng, Yan-Ke Chen, and Liang-Zhen Wen for helpful discussions.

[1] S. Weinberg, Phenomenological Lagrangians, Physica (Amsterdam) **96A**, 327 (1979).
[2] J. Gasser and H. Leutwyler, Chiral perturbation theory to one loop, Ann. Phys. (N.Y.) **158**, 142 (1984).
[3] J. Gasser and H. Leutwyler, Chiral perturbation theory: Expansions in the mass of the strange quark, Nucl. Phys. **B250**, 465 (1985).
[4] S. Weinberg, Nuclear forces from chiral Lagrangians, Phys. Lett. B **251**, 288 (1990).
[5] S. Weinberg, Effective chiral Lagrangians for nucleon-pion interactions and nuclear forces, Nucl. Phys. **B363**, 3 (1991).
[6] E. E. Jenkins and A. V. Manohar, Baryon chiral perturbation theory using a heavy fermion Lagrangian, Phys. Lett. B **255**, 558 (1991).
[7] V. Bernard, N. Kaiser, J. Kambor, and U. G. Meissner, Chiral structure of the nucleon, Nucl. Phys. **B388**, 315 (1992).
[8] T. R. Hemmert, B. R. Holstein, and J. Kambor, Chiral Lagrangians and delta(1232) interactions: Formalism, J. Phys. G **24**, 1831 (1998).
[9] E. Epelbaum, H. W. Hammer, and U. G. Meissner, Modern theory of nuclear forces, Rev. Mod. Phys. **81**, 1773 (2009).
[10] R. Machleidt and D. R. Entem, Chiral effective field theory and nuclear forces, Phys. Rep. **503**, 1 (2011).
[11] L. Meng, B. Wang, G. J. Wang, and S. L. Zhu, Chiral perturbation theory for heavy hadrons and chiral effective field theory for heavy hadronic molecules, Phys. Rep. **1019**, 1 (2023).

[12] R. Aaij *et al.* (LHCb Collaboration), Observation of an exotic narrow doubly charmed tetraquark, Nat. Phys. **18**, 751 (2022).

[13] R. Aaij *et al.* (LHCb Collaboration), Study of the doubly charmed tetraquark T_{cc}^+, Nat. Commun. **13**, 3351 (2022).

[14] A. V. Manohar and M. B. Wise, Exotic Q Q anti-q anti-q states in QCD, Nucl. Phys. **B399**, 17 (1993).

[15] D. Janc and M. Rosina, The $T_{cc} = DD^*$ molecular state, Few Body Syst. **35**, 175 (2004).

[16] S. Ohkoda, Y. Yamaguchi, S. Yasui, K. Sudoh, and A. Hosaka, Exotic mesons with double charm and bottom flavor, Phys. Rev. D **86**, 034019 (2012).

[17] N. Li, Z. F. Sun, X. Liu, and S. L. Zhu, Coupled-channel analysis of the possible $D^{(*)}D^{(*)}$, $\bar{B}^{(*)}\bar{B}^{(*)}$ and $D^{(*)}\bar{B}^{(*)}$ molecular states, Phys. Rev. D **88**, 114008 (2013).

[18] K. Chen, R. Chen, L. Meng, B. Wang, and S. L. Zhu, Systematics of the heavy flavor hadronic molecules, Eur. Phys. J. C **82**, 581 (2022).

[19] R. Chen, Q. Huang, X. Liu, and S. L. Zhu, Predicting another doubly charmed molecular resonance $T_{cc}'^+(3876)$, Phys. Rev. D **104**, 114042 (2021).

[20] X. K. Dong, F. K. Guo, and B. S. Zou, A survey of heavy–heavy hadronic molecules, Commun. Theor. Phys. **73**, 125201 (2021).

[21] A. Feijoo, W. H. Liang, and E. Oset, $D^0D^0\pi^+$ mass distribution in the production of the T_{cc} exotic state, Phys. Rev. D **104**, 114015 (2021).

[22] M. Albaladejo, T_{cc}^+ coupled channel analysis and predictions, Phys. Lett. B **829**, 137052 (2022).

[23] S. Fleming, R. Hodges, and T. Mehen, T_{cc}^+ decays: Differential spectra and two-body final states, Phys. Rev. D **104**, 116010 (2021).

[24] L. Meng, G. J. Wang, B. Wang, and S. L. Zhu, Probing the long-range structure of the T_{cc}^+ with the strong and electromagnetic decays, Phys. Rev. D **104**, 051502 (2021).

[25] M. L. Du, V. Baru, X. K. Dong, A. Filin, F. K. Guo, C. Hanhart, A. Nefediev, J. Nieves, and Q. Wang, Coupled-channel approach to T_{cc}^+ including three-body effects, Phys. Rev. D **105**, 014024 (2022).

[26] H. W. Ke, X. H. Liu, and X. Q. Li, Possible molecular states of $D^{(*)}D^{(*)}$ and $B^{(*)}B^{(*)}$ within the Bethe–Salpeter framework, Eur. Phys. J. C **82**, 144 (2022).

[27] Z. Y. Lin, J. B. Cheng, and S. L. Zhu, T_{cc}^+ and $X(3872)$ with the complex scaling method and $DD(\bar{D})\pi$ three-body effect, arXiv:2205.14628.

[28] J. B. Cheng, Z. Y. Lin, and S. L. Zhu, Double-charm tetraquark under the complex scaling method, Phys. Rev. D **106**, 016012 (2022).

[29] X. Z. Ling, M. Z. Liu, L. S. Geng, E. Wang, and J. J. Xie, Can we understand the decay width of the T_{cc}^+ state?, Phys. Lett. B **826**, 136897 (2022).

[30] Y. Liu, M. A. Nowak, and I. Zahed, Holographic tetraquarks and the newly observed T_{cc}^+ at LHCb, Phys. Rev. D **105**, 054021 (2022).

[31] M. J. Yan and M. P. Valderrama, Subleading contributions to the decay width of the T_{cc}^+ tetraquark, Phys. Rev. D **105**, 014007 (2022).

[32] Y. Jin, S. Y. Li, Y. R. Liu, Q. Qin, Z. G. Si, and F. S. Yu, Color and baryon number fluctuation of preconfinement system in production process and T_{cc} structure, Phys. Rev. D **104**, 114009 (2021).

[33] Q. Xin and Z. G. Wang, Analysis of the doubly-charmed tetraquark molecular states with the QCD sum rules, Eur. Phys. J. A **58**, 110 (2022).

[34] J. Shi, E. Wang, and Q. Wang, Investigating the isospin property of T_{cc}^+ from its Dalitz plot distribution, Phys. Rev. D **106**, 096012 (2022).

[35] P. G. Ortega, J. Segovia, D. R. Entem, and F. Fernandez, Nature of the doubly-charmed tetraquark T_{cc}^+ in a constituent quark model, Phys. Lett. B **841**, 137918 (2023).

[36] M. L. Du, A. Filin, V. Baru, X. K. Dong, E. Epelbaum, F. K. Guo, C. Hanhart, A. Nefediev, J. Nieves, and Q. Wang, Role of left-hand cut contributions on pole extractions from lattice data: Case study for $T_{cc}(3875)^+$, Phys. Rev. Lett. **131**, 131903 (2023).

[37] B. Wang and L. Meng, Revisiting the DD^* chiral interactions with the local momentum-space regularization up to the third order and the nature of T_{cc}^+, Phys. Rev. D **107**, 094002 (2023).

[38] C. Chen, C. Meng, Z. G. Xiao, and H. Q. Zheng, Some remarks on compositeness of T_{cc}^+, Chin. Phys. C **48**, 043102 (2024).

[39] See Supplemental Material at http://link.aps.org/supplemental/10.1103/PhysRevD.109.L071505 for more technical details about the one-pion exchange potential involving the three-body threshold dynamics, an alternative scheme to deal with the singularities of the potential function in the integral, and integral path schemes of solving the on-shell T matrix with a positive real momentum, in addition to which the results of the predicted scattering phase shifts based on the existence of right-hand cut structure and the cut structures of the three-body threshold dynamics with involving the kinetic energy terms of the heavy mesons are presented.

[40] Y. K. Chen, L. Meng, Z. Y. Lin, and S. L. Zhu, Virtual states in the coupled-channel problems with an improved complex scaling method, Phys. Rev. D **109**, 034006 (2024).

[41] Y. Ikeda, B. Charron, S. Aoki, T. Doi, T. Hatsuda, T. Inoue, N. Ishii, K. Murano, H. Nemura, and K. Sasaki, Charmed tetraquarks T_{cc} and T_{cs} from dynamical lattice QCD simulations, Phys. Lett. B **729**, 85 (2014).

[42] S. Chen, C. Shi, Y. Chen, M. Gong, Z. Liu, W. Sun, and R. Zhang, $T_{cc}(3875)$ relevant DD^* scattering from Nf $= 2$ lattice QCD, Phys. Lett. B **833**, 137391 (2022).

[43] M. Padmanath and S. Prelovsek, Signature of a doubly charm tetraquark pole in DD^* scattering on the lattice, Phys. Rev. Lett. **129**, 032002 (2022).

[44] G. K. C. Cheung, C. E. Thomas, J. J. Dudek, and R. G. Edwards (Hadron Spectrum Collaboration), Tetraquark operators in lattice QCD and exotic flavour states in the charm sector, J. High Energy Phys. 11 (2017) 033.

[45] P. Junnarkar, N. Mathur, and M. Padmanath, Study of doubly heavy tetraquarks in lattice QCD, Phys. Rev. D **99**, 034507 (2019).

[46] Y. Lyu, S. Aoki, T. Doi, T. Hatsuda, Y. Ikeda, and J. Meng, Doubly charmed tetraquark T_{cc}^+ from lattice QCD near physical point, Phys. Rev. Lett. **131**, 161901 (2023).